Taylor & Francis
Taylor & Francis Group

ORIGINAL RESEARCH

Check for updates

Identification of novel, immune-mediating extracellular vesicles in human lymphatic effluent draining primary cutaneous melanoma

Rachel L.G. Maus[a], James W. Jakub[b], Tina J. Hieken[b], Wendy K. Nevala[a], Trace A. Christensen[c], Shari L. Sutor[a], Thomas J. Flotte[d], and Svetomir N. Markovic[a]

[a]Department of Oncology, Mayo Clinic, Rochester, MN, USA; [b]Department of Surgery, Mayo Clinic, Rochester, MN, USA; [c]Department of Biochemistry and Molecular Biology, Microscopy and Cell Analysis Core Facility, Mayo Clinic, Rochester, MN, USA; [d]Department of Anatomic and Clinical Pathology, Mayo Clinic, Rochester, MN, USA

ABSTRACT

Epithelial tumors including melanoma often first metastasize to regional, sentinel lymph nodes (SLN). Thus, the presence of SLN metastases is a critical prognostic factor of survival. Prior to metastasis, accumulating evidence suggests the SLN is immunologically compromised; however, the process by which pre-metastatic niche formation occurs remains unknown. In this prospective study, freshly dissected, afferent lymphatic fluid was obtained during SLN biopsy in three patients with primary cutaneous melanoma. Lymphatic extracellular vesicles (L-EV) were visualized by transmission electron microscopy and proteomic cargo profiled by mass spectrometry. Flow cytometry assessed L-EV effects on autologous dendritic cell maturation in vitro. Immunogold electron microscopy and immunohistochemistry visualized expression of EV cargo within the primary tumor and SLN. Lymphatic extracellular vesicles from each afferent lymphatic channel demonstrated inhibition of autologous dendritic cell maturation. Proteomic profiling identified 81 peptides shared among the L-EV preparations including a signature of 18 immune-modulating proteins including previously established inhibitor of dendritic cell maturation, S100A9. Immunohistochemistry and immunogold electron microscopy confirmed S100A9 tracking along the lymphatic path, from keratinocytes in the primary tumor to sub-capsular macrophages in the SLN. Our findings suggest L-EV cargo may serve as early mediators of tumor-induced immune subversion in regional lymph nodes, by preceding malignant cells and trafficking within the lymphatic vasculature to harbor the first pre-metastatic niche.

Introduction

In melanoma, as in most solid tumor malignancies, the most frequent initial site of metastasis is the tumor-draining, sentinel lymph node (SLN).[1,2] Through the use of standard lymphatic mapping techniques, the regional SLN can be reliably traced using intradermal injection of radioactive colloid and an inert blue dye at the site of the primary tumor. As such, excision of the SLN coupled with pathological evaluation for evidence of metastases remains one of the most informative prognostic biomarkers of clinical outcomes and is part of standard of care management of patients with early stage, intermediate thickness, cutaneous melanoma.[3,4] Although the prognostic role of the SLN has been established, human lymphatic circulation remains a largely uncharacterized bio-fluid which only recently is beginning to be profiled for potential biomarkers in various disease types including solid tumor malignancies which primarily utilize the lymphatics for early dissemination. Nevertheless, the capacity of tumor-derived factors within lymphatic fluid to modulate the immune activity of the SLN microenvironment remains unknown.

For a tumor to successfully metastasize, malignant cells must detach from the primary tumor, invade the surrounding lymphatic microvasculature, and induce angiogenesis while simultaneously evading host immune defenses.[5] While inherently inefficient, this process of local invasion and early metastases in epithelial tumors may be sufficiently aided by pre-metastatic conditioning of the SLN. In addition to tumor-induced vascular remodeling,[6–8] accumulating evidence suggests the pre-metastatic niche formation process converts the SLN from an immune organ, primarily responsible for mounting anti-tumor immune responses, to an immunosuppressive microenvironment conducive for metastatic outgrowth. Previous work defining this regionally immunosuppressed landscape in both melanoma and breast cancer has demonstrated compromised dendritic cell (DC) maturation,[9,10] T cell skewing toward chronic inflammation[11] and lymphangiogenesis[12] as features preceding clinical evidence of metastasis in the SLN.

As the cellular and molecular mechanisms responsible for pre-metastatic niche formation continue to be defined, some studies have proposed a critical role for recruited, immature myeloid cells in the pre-metastatic SLN.[13,14] Antigen presentation by mature DCs is required to prime T cells and provide a cytotoxic, anti-tumor immune response.[15] In the pre-metastatic niche setting, recruitment of immature myeloid cells is aided in part by the secretion of chemoattractants, angiogenic and immunosuppressive factors from the primary tumor leading to their accumulation

in the tumor-draining SLN.[16–18] Notably, DC maturation has been shown to be compromised in the SLN of patients with early-stage melanoma in the absence of metastatic disease,[19–21] suggesting a role for subcellular molecules in mediating pre-metastatic niche formation in the SLN.

Cell-derived, membrane-bound extracellular vesicles (EVs) have recently emerged as critical, subcellular immune mediators with both suppressive and activating functions in homeostatic and disease states including cancer.[22] Numerous studies have characterized the proteomic and nucleic cargo associated with EVs identified in peripheral blood,[23] urine,[24] cerebrospinal fluid,[25] and most recently lymphatic leakage.[26,27] In addition to phenotypic characterization of these unique EV subsets, the functional capacity of EVs to modulate recipient cells downstream is actively being explored in metastatic niches.[28] These immunomodulatory effects have also been observed in the pre-metastatic setting, as melanoma exosomes have shown metastasis-promoting properties through recruitment of bone marrow progenitor cells to distant metastatic sites in murine models.[29] Our previous work has demonstrated EVs derived from human melanoma cells inhibit maturation of antigen-presenting DCs *in vitro*, the immune cell subset required for inducing tumor-specific T cell responses.[30] Thus, we postulated that primary cutaneous melanoma may be able to inhibit antigen-presenting functions in the SLN *in vivo*, prior to the arrival of metastasizing melanocytes, through the trafficking of immune-modulatory EVs within afferent lymphatics.

Here, we hypothesize EVs present in the draining lymphatics from the primary tumor contain the molecules capable of aiding in pre-metastatic niche formation in the most frequent, first metastatic site, the SLN. Through extraction of lymph fluid at the time of initial SLN biopsy from the afferent channel draining directly from primary cutaneous melanoma into the SLN in three patients, we characterized lymphatic EVs and evaluated this enriched source of factors from the primary tumor microenvironment for the capacity to traffic and modulate the immune status of the draining SLN, beginning with antigen presentation.

Results

EVs are present in human lymphatic fluid

Confirming our previous observation that vesicular bodies are present in human lymphatic fluid,[30] this study is the first to our knowledge to obtain and characterize the subcellular contents of the afferent lymphatic channel directly upstream of a tumor-draining SLN, identified during SLN mapping. This finding aligns with two recent, independent studies which profiled EVs isolated from the lymphatic exudate allowed to drain through the SLN into the efferent channels, following a positive SLN finding and subsequent lymphadenectomy procedure.[26,27] In the current study, we report findings from three clinical cases (Table 1) in which lymphatic fluid was collected at the time of SLN biopsy rather than the capture post-surgical lymph drainage following lymphadenectomy as previously reported. The clinically standard, lymphatic mapping visualization technique utilizing methylene blue dye was used to ensure the afferent lymphatic ('blue') channel draining from the primary melanoma biopsy site into the SLN was surgically harvested and submitted for fluid extraction (Figure 1a, b). By

Table 1. Summary table of patient demographics and clinical presentation in three patients who underwent SLN biopsy as a part of the clinical management of melanoma.

Patient	1	2	3
Gender	Female	Male	Female
Age	59	51	50
Primary tumor features			
Clark Level	IV	IV	IV
T classification	T2a	T3a	T2a
Breslow depth	1.15	2.9	1.3
Ulceration	No	No	No
Mitotic rate (mm^2)	1	1	2
Radial growth phase	Present	Present	Present
Vertical growth phase	Present	Present	Present
Tumor cell morphology	Epithelioid	Epithelioid and spindled	Epithelioid
Regression	Absent	Absent	Absent
TILs	Non-brisk	Non-brisk	Non-brisk
BRAF status	Not available	Not available	Not available
Following SLN biopsy			
Residual disease in primary	No	No	No
Number of positive SLNs	1	0	0
Number of negative SLNs	1	3	2
Size of largest met	Microscopic clusters positive for Melan A and S100	None	None
Recurrence to date	No	No	No

this approach, a concentrated source of EVs draining directly into the SLN at the time of biopsy is effectively captured. Collecting the lymph directly upstream of the SLN is critical to assessing the initial factors that flow from the primary tumor into the SLN and may potentially influence a pre-metastatic niche. Lymphatic-derived EVs (L-EVs) were identified in the perfused lymphatic fluid of each patient, with vesicle size and composition confirmed by both nanoparticle tracking analysis (Supplemental Figure 1) and immuno-gold labeling for EV-associated cargo Annexin A2 by electron microscopy (Figure 1(c)).

Lymphatic EVs are functionally active and inhibit DC maturation

To assess the functional effects of L-EVs on immune cells, isolated L-EVs were co-cultured with autologous PBMCs. Using a 2-d culture system, peripheral monocytes (CD11c+ DC precursors) within the PBMC culture were stimulated to mature into DCs and expression of cell surface maturation markers CD83 and CD86 were measured by flow cytometry. Both DC-associated CD83 and CD86 expression were significantly compromised in all three patients when co-cultured with autologous L-EVs at the highest dose (2×10^{10} EVs). Notably, at the lower doses (1×10^9 and 1×10^{10} EVs), the L-EVs did not significantly reduce expression of CD83 or CD86 across all patients (Figure 2(a,b)). Monocytes effectively matured into DCs when co-cultured with saline or empty liposomes.

Lymphatic EVs are enriched for pre-metastatic niche promoting factors

With DC maturation compromised in the presence of patient-derived L-EVs, we next performed proteomic profiling by
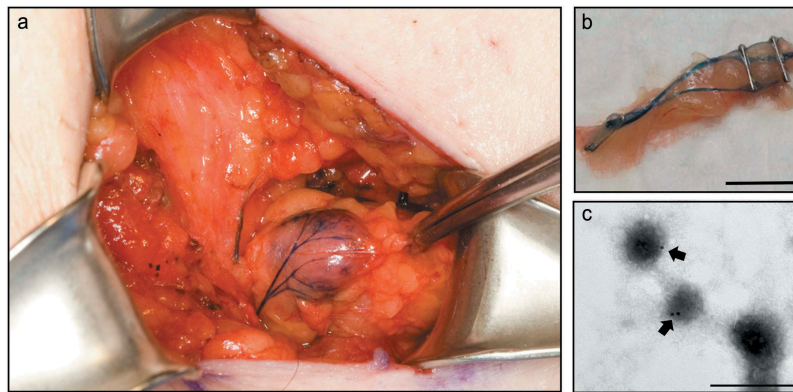
Figure 1. Characterizing primary melanoma lymphatic effluent. (a) During excisional SLN biopsy, the tumor-draining SLN and associated afferent lymphatic channels are visually identified by methylene blue dye staining. (b) In the current study, approximately 1 cm of the afferent lymphatic channel, just proximal to the SLN is surgically dissected and sealed with clips in order to collect lymphatic fluid within the afferent channel (scale bar 0.5 cm). (c) Interrogation of lymphatic fluid following perfusion of the lymphatic channel resulted in the isolation of lymphatic extracellular vesicles (L-EVs) expressing EV-associated marker Annexin A2 by immuno-electron microscopy (scale bar 250 nm) compared to secondary only stained L-EVs (Supplemental Figure 2).
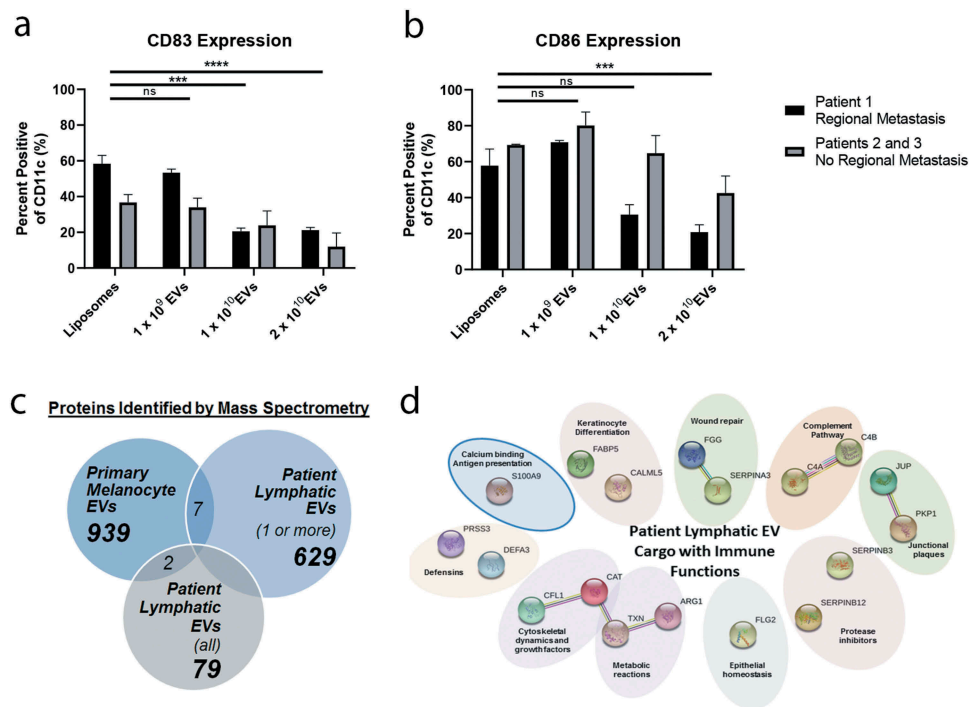

Figure 2. Functional and physiological characterization of human L-EVs. (a and b) L-EVs isolated from each patient were subsequently co-cultured with autologous PBMCs in vitro. Following culture with DC maturation-inducing factors, EV-treated PBMCs exhibited significantly decreased expression of DC maturation markers CD83 and CD86 on CD11c+ DC precursors compared to liposomes alone, in a dose-dependent manner. Co-culture of each patient's PBMCs with autologous L-EVs were conducted in triplicate. (c) Schematic summarizing proteomic assessment of L-EV associated cargo compared to EVs isolated from primary melanocytes by mass spectrometry. (d) Clustering of the 18 candidate L-EV proteins with known immune functions (as determined by NCBI and STRING databases) detected in all L-EV proteomes assessed (n = 3).

mass spectrometry to assess the lymphatic trafficking and immune-modulating potential of the isolated L-EVs. Proteomic profiling revealed 710 total peptide matches expressed in one or more of the three patient L-EV preparations. This L-EV signature was then reduced to 81 peptides detectable in all 3 of the patient EV preparations and contrasted with the proteomic profile of 939 peptides present in EVs isolated from healthy normal melanocytes (*in vitro*), reducing the list to 79 proteins expressed in L-EVs but absent in primary normal melanocyte EVs (Figure 2(c) and

Supplemental Table 1). Further assessment of the L-EV proteomic signatures considered the immune-modulating potential of the vesicles. To determine L-EV cargo with the ability to modulate immunity, the candidate list was searched against the NCBI database, resulting in 18 proteins associated with known innate immune functions (Figure 2d). Clustering these proteins based on their immunological functions, S100A9 emerged as a likely molecule within lymph EVs with the ability to modulate antigen presentation as demonstrated through its overexpression inhibiting DC differentiation in

murine models[31] and its established role as a chemoattractant for human myeloid cells.[32,33]

Lymphatic EV content correlates with protein expression in the primary tumor microenvironment

Given the previously described role of S100A9 in inhibiting DC maturation[31] and its association with melanoma-derived EVs *in vitro*,[30] we next considered the potential of L-EV associated S100A9 originating from the primary tumor site and trafficking to the draining SLN. IHC staining for S100A9 in the primary lesions of patients 1 and 2 revealed the protein was localized primarily to the cytoplasm and nuclei of keratinocytes with patient 1 also demonstrating weak cytoplasmic staining of tumor cells (Figure 3(a,b)). In both cases, the S100A9 staining was localized to the keratinocytes surrounding the primary tumor with decreasing expression in the surrounding stroma. To confirm S100A9 cargo was associating with vesicles trafficking from the primary tumor to the first draining regional lymph node, S100A9 on L-EVs was visualized by immunogold labeling using electron microscopy (Figure 3(c)). S100A9 expression was also detectable in the SLN, displaying a gradient effect, with the most prominent S100A9 staining present in the subcapsular sinus immediately

contiguous with the afferent lymphatic channel with diminishing signal in the more distal, intraparenchymal regions of the lymph node tissue (Figure 3(d,e)). Additionally, S100A9 positive histiocyte staining pattern was observed in some areas of the SLN including the subcapsular sinus (Figure 3(e)) which was further confirmed by IHC staining with macrophage marker CD68 (Figure 3(f)).

This pilot study provides initial evidence of L-EV in the afferent lymphatic fluid collected from three patients undergoing SLN biopsy procedure identifying S100A9 as a potential candidate for further biomarker study. We then expanded our patient cohort to further evaluate the role of S100A9 in determining the metastatic potential of melanoma at the time of SLN biopsy. IHC staining with S100A9 was evaluated in 12 patients (matched for Breslow depth) with or without evidence of recurrence (Table 2). Overall, S100A9 expression was detected in all of the cases assessed however, the staining presented in two distinct patterns. The first was a cytoplasmic stain of primarily histiocytes and CD68+ macrophages (Figure 4(a)) and the second a dark, nuclear stain consistent with dendritic cell staining (Figure 4(b)). Notably, while some cases displayed both staining patterns, the DC staining was present in all but one of the cases that had no evidence of recurrence while cytoplasmic, histiocyte staining was present
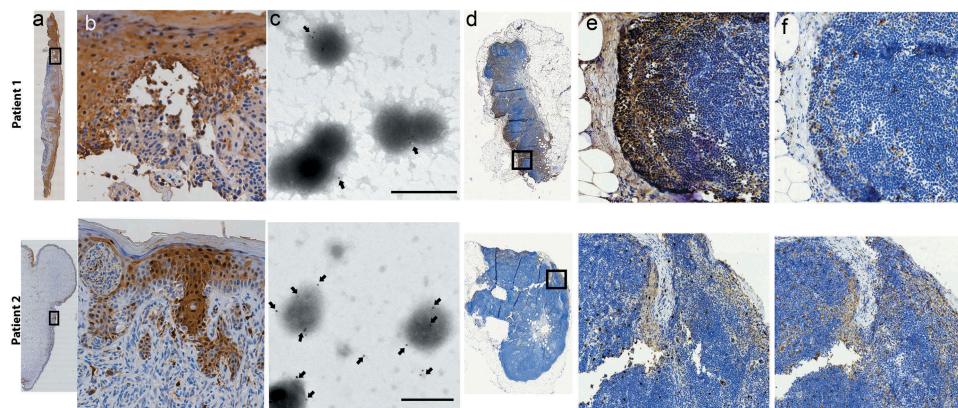

Figure 3. Assessing candidate L-EV cargo S100A9 in the context of lymphatic trafficking.

(a and b, magnification) Immunohistochemical analysis identified cytoplasmic and nuclear S100A9 staining of predominantly keratinocytes in Patients 1 and 2 with additional weak cytoplasmic staining of melanoma cells in Patient 1. (c) By electron microscopy, immunogold labeling with S100A9 (arrows) associated with isolated patient-matched L-EVs (scale bar 250 nm) compared to secondary only stained L-EVs (Supplemental Figure 2). (d and e, magnification) Patient matched SLNs showed expression of S100A9 in a gradient pattern with strongest staining present in the subcapsular sinus as well as S100A9 positive staining in macrophage-enriched areas. Co-localization of S100A9 staining with CD68 macrophage marker was observed on serial tissue section (f).

Table 2. Pathologist scoring of IHC staining with S100A9, CD68, and CD14 on FFPE SLN tissue. S100A9 staining pattern was further defined as cytoplasmic and localized primarily to histiocytes/macrophages or nuclear and localized primarily to dendritic cells.

| Label	Breslow (mm)	Node status	Recurrence	S100A9 (overall)	S100A9 staining pattern Nuclear staining (dendritic cells)	Cytoplasmic staining (histiocytes)	CD68	CD14
SLN1	2.2	Positive	Positive	+++		+++	+++	+++
SLN2	2.4	Positive	Positive	+++		+++	+++	++
SLN3	10	Positive	Positive	+	++	++	++	+
SLN8	1.9	Negative	Positive	++	++	+	++	+
SLN4	0.9	Positive	Negative	+	++	++	++	++
SLN5	0.83	Positive	Negative	+	+++	+	+	+
SLN9	1.15	Positive	Negative	++	+	++	+	+
SLN6	1.3	Negative	Negative	+		+	++	+
SLN10	2.9	Negative	Negative	+	++		+	++
SLN11	8	Negative	Negative	++	+++	++	++	++
SLN12	0.8	Negative	Negative	+	++	++	++	+
SLN13	1.85	Negative	Negative	+	++	++	+	+
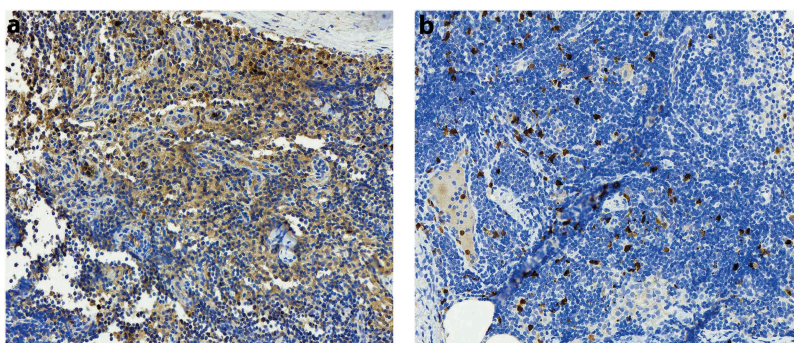
Figure 4. Representative images of S100A9 staining patterns in SLN tissue. IHC staining of S100A9 was observed in all SLN cases assessed and scored by clinical pathologist. Two distinct staining patterns emerged, (a) a cytoplasmic stain correlating with histiocyte regions within the SLN (SLN2) and (b) a nuclear staining of cells consistent with dendritic cells (SLN10).

in all of the cases that had evidence of recurrence. Unlike the correlation with recurrence status, this staining pattern did not correlate with the node status at time of biopsy, suggesting S100A9 may have potential value in the SLN biopsy setting for predicting metastatic potential in addition to the absence/ presence of melanoma cells within the SLN. The results of this small validation cohort provide initial evidence to warrant future studies to evaluate S100A9 and other lymphatic EV cargo candidates as potential predictors of metastatic potential in early disease.

Discussion

As the first site for metastasis among most epithelial tumors, the SLN has increasingly demonstrated elements of immune dysfunction that appear to play a role in its permissiveness to early tumor metastases. Previous work has demonstrated that regional immunosuppression, including compromised DC maturation and vascular remodeling promotes a chronic inflammatory milieu that precedes clinical evidence of metastasis in the SLN.[9-11,19-21] While this compromised phenotype has emerged in both the metastatic and pre-metastatic settings, the factors responsible and the process by which the pre-metastatic niche environment is formed in the SLN remains largely unknown. We therefore chose to interrogate the content of freshly isolated human lymph, draining directly from a cutaneous melanoma and capture the fluid as it enters the SLN via the afferent lymphatic channel, for evidence of subcellular mediators of regional immunosuppression. By collecting lymphatic fluid from this concentrated source immediately downstream of the primary tumor, we were able to sample the factors capable of modulating the recipient SLN and specifically identify candidate factors involved in establishing a pre-metastatic niche. Additionally, by sampling at the time of SLN biopsy, it effectively bypasses the substantial wound healing process associated with post-surgical collection. In this study, we provide evidence supportive of our initial observation that EVs are present in lymphatic fluid[30] and demonstrate for the first time that L-EV is capable of trafficking via the lymphatic vasculature and are functionally equipped to promote pre-metastatic niche formation in the

SLN by inhibiting DC maturation, a prerequisite for antigen presentation and immunologic detection of cancer cells.

Notably, two recent, independent studies characterized EVs collected from the lymphatic leakage following a lymphadenectomy in patients with SLN positive, Stage III metastatic melanoma. Unlike the current study presented which samples a different source along the lymphatic path (surgically dissected afferent lymphatic vessels versus post-surgical lymphatic drainage), Garcia-Silva et al. demonstrated in patients with metastatic disease lymphatic EVs have prognostic utility through the detection of BRAF^{V600E} mutation on the lymphatic EVs[27] and Broggi et al characterized the enrichment of tumor-associated factors including S100 proteins compared to plasma EVs, respectively.[26] While BRAF status was not clinically defined in the patients examined in the current study, future studies considering the influence of BRAF mutation on lymphatic EV cargo has the potential to highlight different mechanisms of action by which regional immunosuppression is mediated in the SLN. These recent findings in downstream lymphatic EVs of patients with advanced stages of metastatic melanoma parallel our findings in the afferent lymphatic channel in patients with early stage disease. As the tumor-associated proteomic EV signature is likely weaker in pre-metastatic, early stage disease, it was critical in this study to identify a concentrated EV source directly downstream of the primary tumor site as it enters the draining SLN. While the surgical technique presented herein requires microdissection capabilities, follow-up validation studies will be critical to evaluate the clinical utility of identifying pre-metastatic niche promoting cargo in the SLN.

To determine the lymphatic factors contributing to pre-metastatic niche formation in the SLN, this study characterized the subcellular fraction of afferent lymphatic fluid draining from primary melanoma lesions into the SLN in three patients. This resulted in the discovery and isolation of lymphatic EVs from an extremely concentrated, albeit low-volume fluid source, collected at the time of SLN biopsy. Standardized EV isolation methodologies remain a challenge for the field at large, especially in studies of low-volume human biofluids in which ultracentrifugation is not feasible. This study provides initial evidence supportive of isolating lymphatic EVs from the afferent channel however future studies evaluating different EV isolation methods including size

exclusion chromatography to further characterize the proteomic and nucleic cargo within lymphatic EVs is warranted.

In addition to trafficking within the lymphatics, L-EV also suggests a functional capacity to interfere with antigen presentation by inhibiting maturation of autologous DCs. These findings align with previous report in pancreatic adenocarcinoma demonstrating pro-tumorigenic effects of miRNA in tumor-derived exosomes including decreased DC maturation and increased DC dysfunction.[34] Taken together, these findings suggest EV-mediated DC dysfunction may be a conserved mechanism employed by tumor and lymphatic-derived EVs to promote immune suppression in different cancer types.

In an effort to identify candidate L-EV cargo capable of mediating this observed effect, 18 proteins with defined roles in immune modulation were found to be present in all L-EV preparations (Figure 2(d)), including S100A9, a myeloid chemoattractant previously shown to inhibit DC maturation.[31] Recently characterized as a damage-associated molecular pattern molecule (DAMP), S100A9 has demonstrated pro-inflammatory properties in both epithelial cells of the skin and the myeloid cell lineage.[35] In tumor-bearing mice, S100A9 has been shown to promote accumulation of myeloid-derived suppressor cells and inhibit DC differentiation.[31] The mechanistic model that is emerging suggests systemic factors including VEGF-A, TGFβ and TNFα are secreted from the primary tumor microenvironment and induce expression of myeloid chemoattractants S100A8 and S100A9 in future metastatic sites.[36] Upregulation of these chemokines in pre-metastatic sites has resulted in the recruitment of immature myeloid cells to the lung in B16 melanoma mouse models to date.[16,37] In this way, an immune-compromised, pre-metastatic niche is initiated by circulating cytokine and chemokines, promoting future metastatic habitats.

In this report, we propose a similar function for S100A9 in the pre-metastatic SLN whereby the lymphatic vasculature is utilized by the primary tumor in order to traffic subcellular factors including L-EV enriched with S100A9 from the primary tumor microenvironment to the pre-metastatic SLN (Figure 5). Our data thus far suggest the source of the L-EVs carrying S100A9 is within the melanoma tumor microenvironment predominantly localizing to the surrounding keratinocytes. This localization aligns with previous studies demonstrating S100A9 expression in melanocytic nevi and melanoma lesions is confined to keratinocytes and epithelium associated with proliferating melanocytes.[38] Notably, Meves et al. evaluated S100A9 expression in skin biopsies by next-generation RNA sequencing, and found primary melanoma tissue demonstrated a significant increase in S100A9 copy number over that of benign nevi (p-value = 0.00423, FDR = 0.0871), further supporting that S100A9 may originate from the microenvironment of the primary tumor and play a predictive role in clinical outcomes of patients with primary melanoma of the skin.[39] While it is plausible S100A9 is directly synthesized by cells within the lymph node, the gradient expression of S100A9 in the subcapsular sinus of the SLN coupled with a recognized, dynamic interaction between melanocytes and neighboring keratinocytes,[40-42] our findings suggest this

interaction at the primary tumor site may be responsible for initiating S100A9-expressing EV secretion into the lymphatics to seed a pre-metastatic niche in the SLN downstream. Future studies evaluating S100A9 expression in normal lymph fluid and lymph nodes are warranted in order to further evaluate the application of S100A9 as a predictor of pre-metastatic niche formation in melanoma and other solid tumors.

As discussions involving the surgical management of regional lymph nodes in patients with melanoma are ongoing, it is increasingly evident that a more comprehensive understanding of the factors responsible for initiating immunological changes to the SLN and regional basin is required. Historically, patients with a positive SLN would proceed to completion lymphadenectomy to determine the extent of regional spread.[40,43] However, recent findings from MSLT-II have demonstrated no survival advantage for patients who underwent completion lymphadenectomy compared to patients who underwent intensive surveillance.[44] Without this surgical intervention to inform therapeutic decision making, there is an urgent need for identification of novel prognostics within the SLN capable of elucidating which patients will benefit from adjuvant treatment and potentially prevent future recurrence.

Upon investigation of fresh, human lymphatic effluent, we have identified a novel source of vesicles which serve as a trafficking mechanism from the primary tumor microenvironment into the first metastatic site, the SLN. Continued evaluation and characterization of the L-EV trafficking mechanisms, the cargo transported and their functional capacity to regulate the SLN immune microenvironment will undoubtedly provide critical insight into the initiating steps of the first pre-metastatic niche.

Materials and methods

Patients

Patient biospecimens were collected in accordance with a biospecimens collection clinical study as approved by the Mayo Clinic Institutional Review Board (IRB: #10-000806). All three patients described were diagnosed with intermediate thickness melanoma and proceeded with SLN biopsy as part of their surgical care. Prior to the SLN biopsy procedure, each patient provided informed consent to participate in a prospective biospecimen study collecting peripheral blood, SLN fresh tissue and an SLN-draining, afferent lymphatic channel as part of the SLN biopsy procedure. The purpose of this study is to identify initiating factors trafficking within the lymphatics and capable of mediating the SLN pre-metastatic niche formation. Despite similar clinical presentations and T-stages, SLN biopsies were negative for tumor metastases in patients 2 and 3, and positive in patient 1 (Table 1). Subsequent IHC analysis was conducted retrospectively on FFPE SLN tissue from 12 additional cases following IRB approval (IRB: #17-004491).

Interrogation of fresh lymph fluid from afferent lymphatic channels

Prior to the SLN biopsy, methylene blue dye was injected intradermally around the primary melanoma biopsy site and
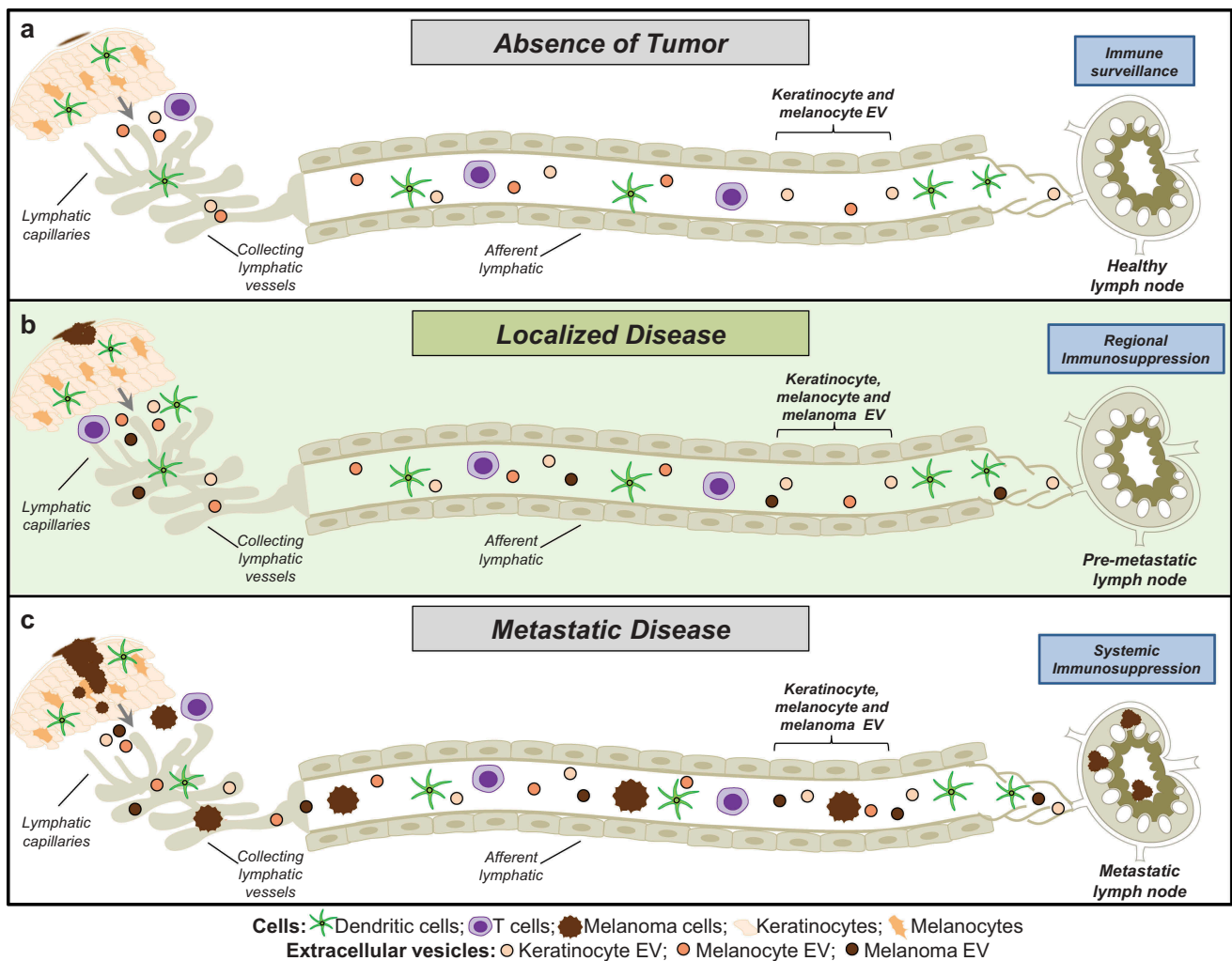
Figure 5. Proposed model of lymphatic trafficking and immune remodeling of the draining SLN. (a) Under homeostatic conditions, interstitial fluid drains into surrounding lymph nodes through a series of lymphatic vessels, transporting soluble proteins, EVs, and circulating immune cells surveying tissues for foreign antigens. (b) In early stage melanoma, malignant cells remain localized to the primary tumor microenvironment; however, in addition to soluble proteins and immune cells, this model demonstrates the afferent lymphatic channel that drains into the proximal SLN also shows enrichment for L-EV potentially derived from resident keratinocytes, melanocytes and melanoma cells of the skin. Results from our study suggest these vesicles promote regional immunosuppression in the pre-metastatic SLN. (c) In the metastatic setting, melanoma cells are capable of trafficking via the lymphatic vasculature, establishing metastatic lesions in the SLN.

allowed 5 min to migrate. Intraoperatively, at the time of the SLN biopsy, an afferent channel was identified entering directly into the SLN via the presence of a blue dye-filled lymphatic. Approximately 1 cm of the afferent lymphatic channel, immediately proximal to the SLN was clipped on both ends, dissected from the surrounding tissue, sharply divided, surgically excised, placed in Roswell Park Memorial Institute (RPMI) media and transported to the lab at ambient temperature. Upon receipt of the fresh specimen, the surgical clips were removed and the fluid within the channel was perfused using a 30 gauge needle with RPMI media and filtered by a 0.8-μm syringe filter prior to vesicle isolation.

Cells and culture conditions

Human adult primary epidermal melanocytes (PCS-200-013; ATCC) were cultured in Dermal Cell Basal Media (PCS-200-030; ATCC) supplemented with Adult Melanocyte growth kit (PCS-200-042; ATCC) and 10U/mL penicillin, 10ug/mL streptomycin

and 10ug/mL gentamicin. Prior to EV isolation, the cells were cultured under hypoxic conditions using Petaka G3 low-oxygen transfer flasks for 48 h at 37°C in a humidified chamber.

Extracellular vesicle (EV) isolation

Extracellular vesicles were isolated from filtered lymphatic fluid (<100 μL) or the conditioned media of cultured healthy, primary melanocytes using exoEasy membrane-affinity spin columns (Qiagen). Commercially available, unloaded liposomes (Sigma) were used at comparable size distribution and total concentration in co-culture experiments, serving as negative control. Quantification of vesicle size distributions and total concentrations was performed using NanoSight NS300 (Malvern, UK).

EV co-culture with peripheral blood mononuclear cells

Peripheral blood mononuclear cells were isolated by Ficoll gradient from whole blood drawn from patients pre-

operatively. Peripheral blood mononuclear cells were co-cultured at 1×10^5 cells/mL with increasing concentrations of autologous lymphatic EVs ($1 \times 10,^9$ 1×10^{10} or 2×10^{10} vesicles/mL), unloaded liposomes (Sigma) or saline. Over a 2-d time course, monocytes within the PBMC culture were stimulated with 20 ng/mL of GM-CSF, IL-4 and 1000 U/mL IFNβ and matured to the DC fate with 10ng/mL TNFα, IL1β, and 1ug/mL PGE2 as previously described.[45] DC maturation was assessed by flow cytometry (Guava, Millipore) by first gating on live cells expressing CD11c monocyte marker (Supplemental Figure 3) and then quantifying the percentage of CD11c+ monocytes with surface expression of maturation markers CD83 and CD86.

Proteomic characterization of lymphatic EV (L-EV) cargo by mass spectrometry

To determine proteomic cargo of the isolated L-EV, purified EVs were concentrated to 50uL total volume and resuspended in 2X lysis buffer (50mM Tris pH 7.4, 150mM NaCl, 1mM EDTA, 0.1% SDS, 1% TX100) supplemented with protease inhibitors, before being separated by 15% SDS-PAGE and visualized by silver stain (ThermoFisher). Healthy primary melanocyte EVs were similarly prepared for comparison. Due to the small starting lymph fraction, protein concentration was not quantified prior to MS assessment but the entire fraction was concentrated and loaded and subjected to a silver stain before segmenting the gel into eight sections as previously described[30] to ensure loading concentrations were comparable (Supplemental Figure 4). Both the primary melanocyte EV and lymphatic EV gels were segmented into eight sections and subjected to liquid chromatography–mass spectrometry performed by the QExactive (Thermo Scientific) coupled to a Thermo Ultimate 3000 RSLCnano HPLC system.

Visualization of L-EVs and associated cargo by electron microscopy

Isolated L-EVs were concentrated by ultrafiltration on 100K filters (Millipore), adhered to carbon-coated 200 mesh Cu grids and immunogold labeled with Annexin A2 (Santa Cruz, sc-28385) or S100A9 antibody (Sigma, HPA004193). Following primary antibody stain, grids were incubated with secondary 10nm gold conjugated antibody or secondary antibody alone. Following a wash in 0.1 M phosphate buffer, pH 7.0, grids were fixed with 4% paraformaldehyde + 1% glutaraldehyde and negatively stained with 1% phosphotungstic acid. Micrographs were acquired using a JEOL1400 Plus transmission electron microscope operating at 80 kV (Peabody, MA).

Immunohistochemical staining of S100A9, CD68, and CD14 in patient tissue

Tissue sectioning and IHC staining with S100A9, CD68, and CD14 were performed at the Pathology Research Core (Mayo Clinic, Rochester, MN) using the Leica Bond RX stainer (Leica). Formalin-fixed, paraffin-embedded (FFPE) tissue from the primary tumor and corresponding SLN were identified for Patients 1 and 2, sectioned at 5 μm and IHC staining was performed. Slides for S100A9 stain were retrieved for 20 min using Epitope Retrieval 1 (Citrate; Leica) and incubated in Protein Block (Dako) for 5 min. The primary antibodies S100A9 (Sigma, HPA004193), CD68 (Dako, PG-M1 clone), and CD14 (Sigma, HPA001887) were diluted to 1:3000, 1:200, and 1:200 in Background Reducing Diluent (Dako) respectively, and incubated for 15 min. The detection system used was a Polymer Refine Detection Kit (Leica). Slides were counterstained with hematoxylin for 5 min followed by serial washes in 1X Bond wash buffer, distilled water and tap water. Slides were dehydrated in increasing concentrations of ethyl alcohol and cleared in three changes of xylene prior to permanent coverslipping in xylene-based medium. The immunostaining results were assessed by an expert, clinical pathologist to determine localization patterns in each case.

Declaration of interest

No conflict of interest disclosures were reported for any of the authors.

References

1. Leong SP. Paradigm of metastasis for melanoma and breast cancer based on the sentinel lymph node experience. Ann Surg Oncol. 2004;11:192S–197S.
2. Reintgen D, Cruse CW, Wells K, Berman C, Fenske N, Glass F, Schroer K, Heller R, Ross M, Lyman G, et al. The orderly progression of melanoma nodal metastases. Ann Surg. 1994;220 (6):759–767. PMCID PMC1234478. doi:10.1097/00000658-199412000-00009.
3. Morton DL, Thompson JF, Cochran AJ, Mozzillo N, Elashoff R, Essner R, Nieweg OE, Roses DF, Hoekstra HJ, Karakousis CP, et al. Sentinel-node biopsy or nodal observation in melanoma. N Engl J Med. 2006;355(13):1307–1317. doi:10.1056/NEJMoa060992.
4. Morton DL, Thompson JF, Cochran AJ, Mozzillo N, Nieweg OE, Roses DF, Hoekstra HJ, Karakousis CP, Puleo CA, Coventry BJ, et al. Final trial report of sentinel-node biopsy versus nodal observation in melanoma. N Engl J Med. 2014;370(7):599–609. PMCID PMC4058881.
5. Martin TA, Ye L, Sanders AJ, Lane J, Jiang WG Cancer invasion and metastasis: molecular and cellular perspective. Madame Curie Bioscience Database [Internet]: Landes Bioscience; 2013.
6. Farnsworth RH, Lackmann M, Achen MG, Stacker SA. Vascular remodeling in cancer. Oncogene. 2014;33:3496–3505.
7. Hirakawa S, Kodama S, Kunstfeld R, Kajiya K, Brown LF, Detmar M. VEGF-A induces tumor and sentinel lymph node lymphangiogenesis and promotes lymphatic metastasis. J Exp Med. 2005;201(7):1089–1099. PMCID PMC2213132.
8. CN Q, Berghuis B, Tsarfaty G, Bruch M, EJ K, Ditlev J, Tsarfaty I, Hudson E, DG J, Petillo D, et al. Preparing the "soil": the primary tumor induces vasculature reorganization in the sentinel lymph

node before the arrival of metastatic cancer cells. Cancer Res. 2006;66:10365–10376.

9. Mansfield AS, Heikkila P, von Smitten K, Vakkila J, Leidenius M. Metastasis to sentinel lymph nodes in breast cancer is associated with maturation arrest of dendritic cells and poor co-localization of dendritic cells and CD8+ T cells. Virchows Arch. 2011;459:391–398.

10. Mansfield AS, Holtan SG, Grotz TE, Allred JB, Jakub JW, Erickson LA, Markovic SN. Regional immunity in melanoma: immunosuppressive changes precede nodal metastasis. Mod Pathol. 2011;24(4):487–494. doi:10.1038/modpathol.2010.227.

11. Grotz TE, Jakub JW, Mansfield AS, Goldenstein R, Enninga EA, Nevala WK, Leontovich AA, Markovic SN. Evidence of Th2 polarization of the sentinel lymph node (SLN) in melanoma. Oncoimmunology. 2015;4(8):e1026504. PMCID PMC4570120. doi:10.1080/2162402X.2015.1008371.

12. Harrell MI, Iritani BM, Ruddell A. Tumor-induced sentinel lymph node lymphangiogenesis and increased lymph flow precede melanoma metastasis. Am J Pathol. 2007;170 (2):774–786. PMCID PMC1851877. doi:10.2353/ ajpath.2007.060761.

13. Gil-Bernabe AM, Ferjancic S, Tlalka M, Zhao L, Allen PD, Im JH, Watson K, Hill SA, Amirkhosravi A, Francis JL, et al. Recruitment of monocytes/macrophages by tissue factor-mediated coagulation is essential for metastatic cell survival and premetastatic niche establishment in mice. Blood. 2012;119(13):3164–3175. doi:10.1182/blood-2011-08-376426.

14. Liu Y, Cao X. Characteristics and significance of the pre-metastatic niche. Cancer Cell. 2016;30(5):668–681. doi:10.1016/j.ccell.2016.09.011.

15. Gardner A, Ruffell B. Dendritic cells and cancer immunity. Trends Immunol. 2016;37(12):855–865. PMCID PMC5135568. doi:10.1016/j.it.2016.09.006.

16. Hiratsuka S, Watanabe A, Sakurai Y, Akashi-Takamura S, Ishibashi S, Miyake K, Shibuya M, Akira S, Aburatani H, Maru Y. The S100A8-serum amyloid A3-TLR4 paracrine cascade establishes a pre-metastatic phase. Nat Cell Biol. 2008;10 (11):1349–1355. doi:10.1038/ncb1794.

17. Kowanetz M, Wu X, Lee J, Tan M, Hagenbeek T, Qu X, Yu L, Ross J, Korsisaari N, Cao T, et al. Granulocyte-colony stimulating factor promotes lung metastasis through mobilization of Ly6G +Ly6C+ granulocytes. Proc Natl Acad Sci U S A. 2010;107 (50):21248–21255. PMCID PMC3003076. doi:10.1073/ pnas.1015855107.

18. Qian BZ, Li J, Zhang H, Kitamura T, Zhang J, Campion LR, Kaiser EA, Snyder LA, Pollard JW. CCL2 recruits inflammatory monocytes to facilitate breast-tumour metastasis. Nature. 2011;475(7355):222–225. PMCID PMC3208506. doi:10.1038/ nature10138.

19. Cochran AJ, Morton DL, Stern S, Lana AM, Essner R, Wen DR. Sentinel lymph nodes show profound downregulation of antigen-presenting cells of the paracortex: implications for tumor biology and treatment. Mod Pathol. 2001;14(6):604–608. doi:10.1038/modpathol.3880358.

20. Essner R, Kojima M. Dendritic cell function in sentinel nodes. Oncology (Williston Park). 2002;16:27–31.

21. Ferris RL, Lotze MT, Leong SP, Hoon DS, Morton DL. Lymphatics, lymph nodes and the immune system: barriers and gateways for cancer spread. Clin Exp Metastasis. 2012;29 (7):729–736. PMCID PMC3485421. doi:10.1007/s10585-012-9520-2.

22. Thery C, Ostrowski M, Segura E. Membrane vesicles as conveyors of immune responses. Nat Rev Immunol. 2009;9(8):581–593. doi:10.1038/nri2567.

23. Revenfeld AL, Baek R, Nielsen MH, Stensballe A, Varming K, Jorgensen M. Diagnostic and prognostic potential of extracellular vesicles in peripheral blood. Clin Ther. 2014 Epub 2014/ 06/24;36 (6):830–846. doi:10.1016/j.clinthera.2014.05.008.

24. Barreiro K, Holthofer H. Urinary extracellular vesicles. A promising shortcut to novel biomarker discoveries. Cell

Tissue Res. 2017;369(1):217–227. Epub 2017/ 04/22 PMCID PMC5487850 doi:10.1007/s00441-017-2621-0

25. Welton JL, Loveless S, Stone T, von Ruhland C, Robertson NP, Clayton A. Cerebrospinal fluid extracellular vesicle enrichment for protein biomarker discovery in neurological disease; multiple sclerosis. J Extracell Vesicles. 2017;6(1):1369805. Epub 2017/ 09/ 30 PMCID PMC5614217 doi:10.1080/20013078.2017.1369805

26. Broggi MAS, Maillat L, Clement CC, Bordry N, Corthesy P, Auger A, Matter M, Hamelin R, Potin L, Demurtas D, et al. Tumor-associated factors are enriched in lymphatic exudate compared to plasma in metastatic melanoma patients. J Exp Med. 2019;216(5):1091–1107. Epub 2019/ 04/13 PMCID PMC6504224 doi:10.1084/jem.20181618

27. Garcia-Silva S, Benito-Martin A, Sanchez-Redondo S, Hernandez-Barranco A, Ximenez-Embun P, Nogues L, Mazariegos MS, Brinkmann K, Amor Lopez A, Meyer L, et al. Use of extracellular vesicles from lymphatic drainage as surrogate markers of melanoma progression and BRAF (V600E) mutation. J Exp Med. 2019 Epub 2019/ 04/13;216(5):1061–1070. doi:10.1084/jem.20181522.

28. Gener Lahav T, Adler O, Zait Y, Shani O, Amer M, Doron H, Abramovitz L, Yofe I, Cohen N, Erez N. Melanoma-derived extracellular vesicles instigate proinflammatory signaling in the metastatic microenvironment. Int J Cancer. 2019;Epub 2019/ 06/20. doi:10.1002/ijc.32521.

29. Peinado H, Aleckovic M, Lavotshkin S, Matei I, Costa-Silva B, Moreno-Bueno G, Hergueta-Redondo M, Williams C, Garcia-Santos G, Ghajar C, et al. Melanoma exosomes educate bone marrow progenitor cells toward a pro-metastatic phenotype through MET. Nat Med. 2012;18(6):883–891. PMCID PMC3645291. doi:10.1038/ nm.2753.

30. Maus RLG, Jakub JW, Nevala WK, Christensen TA, Noble-Orcutt K, Sachs Z, Hieken TJ, Markovic SN. Human melanoma-derived extracellular vesicles regulate dendritic cell maturation. Front Immunol. 2017;8:358. PMCID PMC5372822. doi:10.3389/fimmu.2017.00358.

31. Cheng P, Corzo CA, Luetteke N, Yu B, Nagaraj S, Bui MM, Ortiz M, Nacken W, Sorg C, Vogl T, et al. Inhibition of dendritic cell differentiation and accumulation of myeloid-derived suppressor cells in cancer is regulated by S100A9 protein. J Exp Med. 2008;205(10):2235–2249. PMCID PMC2556797.

32. Hobbs JA, May R, Tanousis K, McNeill E, Mathies M, Gebhardt C, Henderson R, Robinson MJ, Hogg N. Myeloid cell function in MRP-14 (S100A9) null mice. Mol Cell Biol. 2003;23 (7):2564–2576. PMCID PMC150714.

33. Lackmann M, Rajasekariah P, Iismaa SE, Jones G, Cornish CJ, Hu S, Simpson RJ, Moritz RL, Geczy CL. Identification of a chemotactic domain of the pro-inflammatory S100 protein CP-10. J Immunol. 1993;150:2981–2991.

34. Whiteside TL. The effect of tumor-derived exosomes on immune regulation and cancer immunotherapy. Future Oncol. 2017;13 (28):2583–2592. Epub 2017/ 12/05 PMCID PMC5827821

35. Kerkhoff C, Voss A, Scholzen TE, Averill MM, Zanker KS, Bornfeldt KE. Novel insights into the role of S100A8/A9 in skin biology. Exp Dermatol. 2012;21(11):822–826. PMCID PMC3498607.

36. Rafii S, Lyden D. S100 chemokines mediate bookmarking of premetastatic niches. Nat Cell Biol. 2006;8(12):1321–1323. PMCID PMC2955889.

37. Hiratsuka S, Nakamura K, Iwai S, Murakami M, Itoh T, Kijima H, Shipley JM, Senior RM, Shibuya M. MMP9 induction by vascular endothelial growth factor receptor-1 is involved in lung-specific metastasis. Cancer Cell. 2002;2:289–300.

38. Petersson S, Shubbar E, Enerback L, Enerback C. Expression patterns of S100 proteins in melanocytes and melanocytic lesions. Melanoma Res. 2009;19:215–225.

39. Meves A, Nikolova E, Heim JB, Squirewell EJ, Cappel MA, Pittelkow MR, Otley CC, Behrendt N, Saunte DM, Lock-Andersen J, et al. Tumor cell adhesion as a risk factor for sentinel lymph node metastasis in primary cutaneous melanoma. J Clin Oncol. 2015;33(23):2509–2515. PMCID PMC4979232.

40. Ando H, Niki Y, Ito M, Akiyama K, Matsui MS, Yarosh DB, Ichihashi M. Melanosomes are transferred from melanocytes to

keratinocytes through the processes of packaging, release, uptake, and dispersion. J Invest Dermatol. 2012;132:1222–1229.

41. Valyi-Nagy IT, Hirka G, Jensen PJ, Shih IM, Juhasz I, Herlyn M. Undifferentiated keratinocytes control growth, morphology, and antigen expression of normal melanocytes through cell-cell contact. Lab Invest. 1993;69:152–159.

42. Wang JX, Fukunaga-Kalabis M, Herlyn M. Crosstalk in skin: melanocytes, keratinocytes, stem cells, and melanoma. J Cell Commun Signal. 2016;10(3):191–196. PMCID PMC5055506.

43. Morton DL, Cochran AJ, Thompson JF, Elashoff R, Essner R, Glass EC, Mozzillo N, Nieweg OE, Roses DF, Hoekstra HJ, et al., Multicenter Selective Lymphadenectomy Trial G. Sentinel node biopsy for early-stage melanoma: accuracy and morbidity in MSLT-I, an international multicenter trial. Ann Surg. 2005;242(3):302–311. discussion 311-303PMCID PMC1357739

44. Faries MB, Thompson JF, Cochran AJ, Andtbacka RH, Mozzillo N, Zager JS, Jahkola T, Bowles TL, Testori A, Beitsch PD, et al. Completion Dissection or Observation for Sentinel-Node Metastasis in Melanoma. N Engl J Med. 2017;376(23):2211–2222. PMCID PMC5548388.

45. Kodama A, Tanaka R, Saito M, Ansari AA, Tanaka Y. A novel and simple method for generation of human dendritic cells from unfractionated peripheral blood mononuclear cells within 2 days: its application for induction of HIV-1-reactive CD4(+) T cells in the hu-PBL SCID mice. Front Microbiol. 2013;4:292. PMCID PMC3784773.